Available online at www.sciencedirect.com

ScienceDirect

Energy Procedia 45 (2014) 268 – 277

Energy Procedia

68th Conference of the Italian Thermal Machines Engineering Association, ATI2013

Thermoelectric cells cogeneration from biomass power plant

Augusto Bianchini, Marco Pellegrini, Cesare Saccani*

Department of Industrial Engineering, University of Bologna,Viale Risorgimento 2, Bologna 40124, Italy

Abstract

A thermoelectric cells test facility has been designed and realized at the laboratory of the Department of Industrial Engineering (DIN), University of Bologna. The test facility has been configured to reproduce, in scale, the working conditions of a typical biomass power plant. Commercial thermoelectric cells (also named Seebeck cells) are characterized by direct low efficiency (up to 5%) conversion from thermal to electric energy. Many technical items have to be analyzed and consequent proper solutions must be found to reach the maximum power output. Thus, the test facility will return a great deal of information as regards the best integration between cells and biomass power plant. Furthermore, due to low cell efficiency, the goal of the integration is not to produce electrical energy for external power supply, but to realize a stand-alone biomass power plant wherein the electrical energy produced is totally auto-consumed. The paper shows the test facility and the experimental results and introduces the new test device that has been designed for industrial application.

Keywords: Thermoelectric cells; biomass boiler; cogeneration; test facility.

1. Introduction

Thermoelectric conversion is the result of a process by which heat is converted directly into electricity (Seebeck effect) and, besides occurring in simple thermocouples, forms the basis of thermoelectric generators (TEGs, also named Seebeck cells). Thermoelectric power generation has the advantages of being substantially maintenance free, silent in operation and involving no moving or complex parts. The efficiency of conversion has not managed to exceed 5% for temperature ranges of practical interest. Thus, power generation applications have in the past been limited to special applications, like deep space probes, remote power for Polar Regions or petroleum platforms.

* Corresponding author. Tel.: +39-051-2093404; fax: +39-051-2093404.
E-mail address: cesare.saccani@unibo.it

doi:10.1016/j.egypro.2014.01.029

Currently, fossil fuels such as oil, coal and natural gas represent the prime energy sources in the world. However, a shift towards utilizing a variety of renewable energy resources (RES), which are less environmentally harmful such as solar, wind or biomass in a sustainable way, has taken place in the last few years. Biomass is one of the earliest sources of energy, especially in rural areas where it is often the only accessible and convenient source of energy. Compared to other renewable technologies such as solar or wind energy, biomass has few problems with energy storage because, in a sense, biomass is stored energy. Furthermore, biomass is a versatile fuel that can be used as biogas, liquid fuel or solid fuel. However, in order to further increase the share of energy produced from biomass plants, it is necessary to improve critical issues that limit their spread and efficiency. In particular, the limits that are identified as the most determining, especially for plant size under 350 kWth (i.e. residential or domestic), are difficulties and/or high costs of connection to the grid in the case of isolated installations (a solution which is indeed quite frequent in the case of biomass boilers) and security system reliability in the event of power failure or sudden stop [1]. Integration of TEGs with a biomass boiler makes it possible to increase efficiency (the biomass boiler becomes a cogeneration plant) and produce electricity. Thus, by appropriate dimensioning it is possible to produce the electrical energy required for boiler auto-consumption, so making it unnecessary to connect it to the grid and ensuring greater reliability of the system even in the case of black-out.

Nomenclature

A	Cross area of the thermoelement [m^2]	T_{HF}	Hot fluid average temperature [K]
DIN	Department of Industrial Engineering	T_H	TEG hot temperature [K]
L	Length (also called height) of thermoelement [m]	T_{HC}	Computed TEG hot temperature [K]
L_C	Thickness of solder/contact in the module [m]	T_H'	Measured hot temperature [K]
m	Electrical load ratio	TEG	Thermoelectric Generator
n	Resistivity contact parameter	V_{OC}	TEG open circuit voltage [V]
N	Number of thermoelements per module		
P	Power [W]	α	TEG Seebeck coefficient [V/K]
r	Conductivity contact parameter	ΔT	Hot-cold TEG temperature difference [K]
R	Electrical resistance of thermoelectric generator [Ω]	ε_λ	Conductivity factor
R_L	Load electrical resistance [Ω]	ε_S	Surface heat uniformity factor
RES	Renewable Energy Resources	ρ	TEG electric resistivity [Ωm]
T_{CF}	Cold fluid average temperature [K]	ρ_C	Contact electric resistivity [Ωm]
T_C	TEG cold temperature [K]	λ	TEG thermal conductivity [W/mK]
T_{CC}	Computed TEG cold temperature [K]	λ_C	Contact thermal conductivity [W/mK]
T_C'	Measured cold temperature [K]	η	TEG conversion efficiency

The paper shows the test facility realized at the laboratory of the Department of Industrial Engineering, University of Bologna, to study TEG performance, the experimental results and the new test device that has been designed for industrial application.

2. Thermoelectric power generation from biomass

2.1. Thermoelectric background

The thermoelectric effect was discovered by Seebeck in 1822: he observed an electric flow when one junction of two dissimilar metals, joined at two places, was heated while the other junction was kept at lower temperature. The electrical output produced was initially of small magnitude. After the discovery of semiconductors, it was found that the output could be significantly increased and thus interest in the Seebeck effect was revived around the middle of the 20th century.

A Typical TEG (see Figure 1) is composed of a set of semiconductor components formed from two different materials that are connected thermally in parallel and electrically in series. Moreover, two ceramic plates are attached on each side for electrical insulation. When heat flows through the cell, the N-type components are loaded negatively (excess of electrons) and P-type components are loaded positively (default electron), resulting in the formation of an electric flow. The parameter giving the output voltage for a given p-n junction and for a certain temperature difference between hot and cold side is the "Seebeck coefficient" α. Seebeck coefficients of metals are in the range 0-50 μV/K, while for semiconductors they can be over 300 μV/K [2].

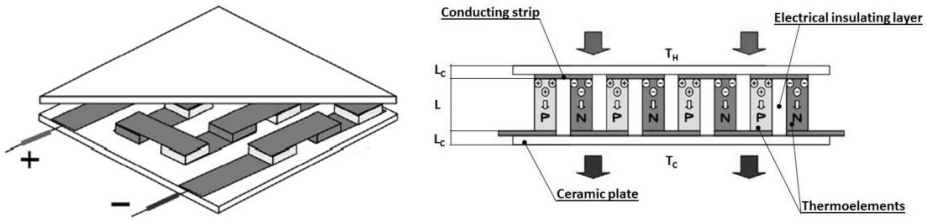

Fig. 1. (a) Thermoelectric generator; (b) Thermoelectric generator cross section.

When the effects of thermal and electrical contact resistances are taken into consideration [2], the power output P of the TEG is given by Equation 1, where m, n and r are, respectively, the ratio between load electric resistance and thermoelectric module electric resistance ($m=R_L/R$), the ratio between contact resistivity and thermoelectric module resistivity ($n=\rho_C/\rho$) and the ratio between contact conductivity and thermoelectric module conductivity ($r=\lambda_C/\lambda$).

$$P = \frac{2m}{(1+m)^2}\frac{\alpha^2}{\rho}\frac{NA(T_H - T_C)^2}{(L+n)(1+2rL_C/L)} \tag{1}$$

So, power output depends upon electric load (m), temperature difference applied (T_H-T_C), thermocouple materials (α and ρ), module geometry (A, N , L and L_C, defined in nomenclature) and module fabrication process (n and r). Equation 1 clearly shows that, regardless of other factors, optimization occurs when m=1 (matched load). In this work, the open-circuit voltage is also assessed; this is easily given from the definition of Seebeck effect by Equation 2.

$$V_{OC} = 2\alpha N(T_H - T_C) \tag{2}$$

Measurements of the TEG conversion efficiency η (i.e. the ratio between electrical power output and heat input) presents difficulties because it requires an accurate determination of the heat input absorbed at its hot side. However, a realistic estimation has been proposed [2], showing that highest power would be not at the highest efficiency [3]. Thus, an equilibrium between maximum power and maximum efficiency must be found depending on specific application.

2.2. State of the art of thermoelectric generation from biomass combustion

Since heat sources for thermoelectric generation feeding are expensive (i.e. fossil fuel), improvements are still needed because only higher conversion efficiency can improve the economic viability of the thermoelectric module. Instead, when heat recovery is essentially free (waste heat), a significant improvement can be obtained by both power per unit area increase and reduction in fabrication cost, ignoring TEG low conversion efficiency. Thus, the application of TEG as both generator and heat exchanger seems to be the best solution [4]. In fact, in this case when

heat flows through TEG, part of the heat absorbed is converted into electricity, while the rest, instead of being discharged into the environment, is collected and used in a heat exchange system. If biomass boiler integration with TEGs is considered, other relevant advantages occur. First of all, connection to the electrical grid in the case of isolated installations, that is quite frequent in the case of biomass residential or domestic plants, can be a major economical obstacle to the biomass plant realization. Moreover, integration between TEGs and a biomass boiler increases system safety, because auxiliary systems that require electrical power can be supplied even in the absence of electrical energy by the grid.

The first stove biomass generator was developed in Sweden in 1996 [5] to provide small amounts of power to homes in the remote northern areas of the country which were beyond the electric grid. Mean working condition were stove surface temperature of about 200°C and heat sink temperature of about 75°C: in these conditions, the two TEGs connected in series (HZ-20 model) were able to produce a gross power of about 10 W (5 W for each). Heat sink was cooled by a 2.2 W fan. Moreover, the Swedish study focuses on a DC/DC converter that, at low power output, is indispensable to increase output voltage, but with consistent power loss. Another important experiment was carried out in Lebanon [6], where three TEGs connected in series (HZ-20 model) were integrated in a wood domestic stove and tested: the final results (comparable with [5]) are a maximum power output of 4.2 W for each TEG at a condition of stove surface temperature of 275°C and heat sink temperature of 123°. In this case, the TEG was naturally cooled. Furthermore, the study demonstrates how for a given heat sink and heat source, increasing the number of TEGs can decrease power output although higher voltages can be realized. Finally, a different cooling system was tested [7]: a heat sink composed of thermosyphonic heat pipe was tested on a HZ-20 TEG, producing about 3 W of power with a temperature of 102°C on heat sink and a temperature of 212°C on hot surface, that was heated by a gas burner. Similar experiments were carried out in Thailand [8] and France [9,10] with the use of different commercially available TEGs but comparable in terms of electrical power output and working conditions.

A test facility has been set up in the DIN Laboratory in order to carry out in-depth studies on the functioning of TEGs and verify performance changes under certain design parameters.

3. Test facility set-up

The first design decision involved the identification of a commercial TEG to be tested. The choice fell on the HZ-20 module, both because it has interesting technical features (power output and conversion efficiency) compared to other commercial modules, and because data are present in the literature [3,5,6,7] on the productive capacity of this module, thus allowing a comparison with the present study. Table 1 gives a listing of the major features of the HZ-20 module [7]: the module, under design temperatures (T_H=230°C, T_C=30°C) and matched load, provides a minimum of 19 W.

Table 1. Specifications and properties of the HZ-20 module.

Thermoelectrical material	Bismuth Telluride (n/p)
Weight (g)	115
Module dimensions (mm)	75x75x5.08
Number of couples N	71
Maximum hot operating temperature T_H (°C)	250
Thermal conductivity λ (W/mK)	2.4
Internal electric resistance R (Ω)	0.3

As shown by Equation 1, once a TEG is chosen, the only parameters that can affect power output are electrical load ratio and temperature difference between hot and cold junctions. Under matched load conditions, the HZ-20 module power output follows the ratio of Figure 2 [7], where $P=5.0\times10^{-4}\times\Delta T^2$. HZ-20 module open circuit voltage V_{OC} can be expressed as a temperature difference function too: $V_{OC}=0.026\times\Delta T$ [7].

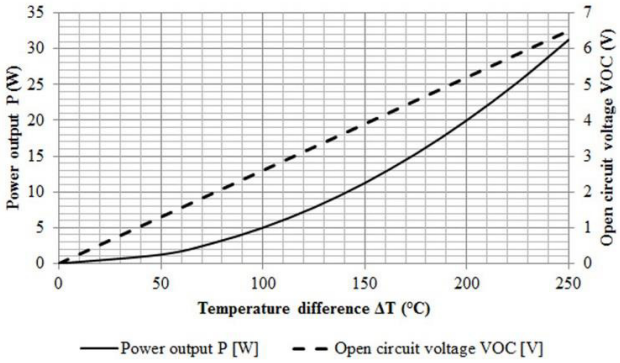

Fig. 2. HZ-20 module power output P and open circuit voltage V_{OC} as a function of temperature difference ΔT under matched load conditions.

The test facility was realized with the aim of studying TEGs performance under different working conditions [11]. A schematic of the heat transfer system is shown in Figure 3. The module is compressed between two stainless steel plates: the clamping force is adjusted by means of four bolts. A heat flow is supplied to the bottom plate. It is obtained by one or more industrial heat guns able to supply heat air from 90°C to 630°C with flow rate from 300 l/min to 500 l/min for each gun. Industrial heat guns simulate flow gas produced by biomass combustion inside the boiler combustion chamber. The top plate is cooled by water: water flow rate is regulated by control manual valves. The temperatures are measured on the top and bottom plates by K type thermocouples (one thermocouple for each one). The whole system is covered by a thermal insulator to limit heat dispersions in the environment. In order to test TEG power output P dependence on R_L variation, an electrical circuit was realized as TEG load where resistance can be set at different values.

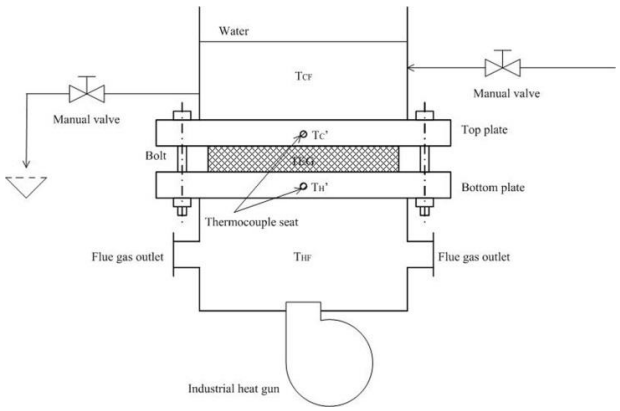

Fig. 3. Schematic overview of the test facility.

Different test facility set-ups were tested: first of all, attention was focused on surface contact between TEG and both top and bottom plates. In particular, tests were carried on with rough surface plates and then with ground surface to measure surface quality influence on TEG performance. Secondly, the system was tested with and without ceramic wafer. Furthermore, plates of aluminum and thermal grease were added between the TEG and both top and bottom ceramic wafers: their influence on TEG performance was investigated. Moreover, tests were conducted with different degrees of bolt fastening (regulated by a torque wrench) to evaluate TEG compression influence. Finally, R_L was also changed. Table 2 summarizes the set-up characteristics. Data were collected in different steady-state conditions thanks to the opportunity of regulating flue gas temperature and flow and water flow. So, power output P and open circuit voltage V_{OC} were measured as a function of temperature variation on test facility top and bottom plates.

Table 2. Test facility set-up characterization.

Test facility set-up	Plate surface quality	Ceramic wafer	Aluminum plate and thermal grease	TEG compression (bar)	R_L (Ω)
01	Rough	No	No	27.6	0.25
02	Ground	No	No	27.6	0.25
03	Ground	Yes	No	13.8	0.25
04	Ground	Yes	No	13.8	0.30
05	Ground	Yes	No	13.8	0.36
06	Ground	Yes	No	13.8	0.43
07	Ground	Yes	No	27.6	0.36
08	Ground	Yes	Yes	13.8	0.40
09	Ground	Yes	Yes	20.7	0.40
10	Ground	Yes	Yes	27.6	0.40

It should be noted that the measured temperatures T_H' and T_C' does not correspond to the TEG temperature T_H and T_C. In fact, due to the thermal conductivity of stainless steel plates and of ceramic wafers, aluminium plates and thermal grease (see Table 3), if present, T_H and T_C are respectively lower and higher than the measured values, T_H' and T_C'. For example, Figure 4 shows how hot and cold temperature on the TEG sides can be predicted for a system with ceramic wafers and measured hot temperature of 210°C and cold temperature of 30°C: in this case, the computed temperature T_{HC} on the hot side of the TEG is about 195°C, while on the cold side the computed temperature T_{CC} is about 45°C. So, measured temperatures T_H' and T_C' can be converted to computed values of hot and cold temperature on the module side T_{HC} and T_{CC} by a conductivity factor ε_λ that depends on thickness and thermal conductivity of the heat exchange structure. The conductivity factor is defined by Equation 3.

Computed TEG temperature difference is then matched with real TEG temperature difference, that is measured on the basis of V_{OC}, the relationship between V_{OC} and ΔT being known (see Equation 2): in this case, TEG works as a ΔT meter. Finally, surface heat uniformity factor ε_S is defined (see Equation 4) as the ratio between computed temperatures difference (T_{HC}-T_{CC}) and real temperatures difference (T_H-T_E) between TEG's hot and cold sides.

$$\varepsilon_\lambda = \frac{T_{HC} - T_{CC}}{T_H' - T_C'} \tag{3}$$

$$\varepsilon_S = \frac{T_H - T_C}{T_{HC} - T_{CC}} \tag{4}$$

Table 3. TEG, stainless steel plates, ceramic wafer, thermal grease and aluminum plate characteristics.

Element	Thickness (mm)	Thermal conductivity (W/mK)
TEG	5.08	2.4
Stainless steel plates	5.00	70
Ceramic wafer (96% Al_2O_3)	1.50	15
Aluminum plate	3.00	204
Thermal grease (estimated)	0.30	0.77

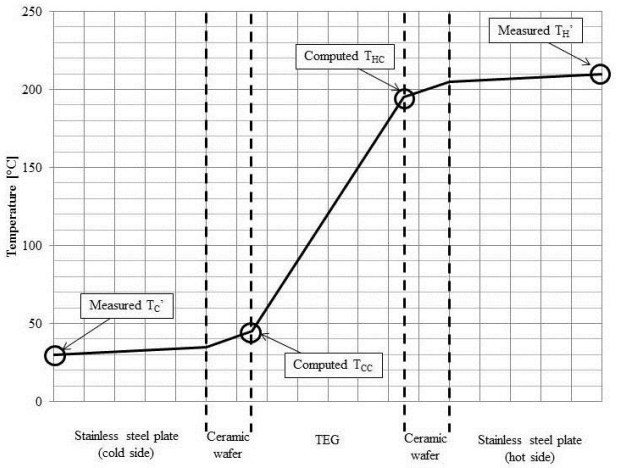

Fig. 4. Difference between computed T_{HC} and T_{CC} and measured T_H and T_C temperatures due to material thermal conductivity in the case of tests with ceramic wafers (no aluminum plate and thermal grease).

4. Test facility results and discussion

Set-up n. 02 differs from n. 01 only for stainless steel plate surface higher quality. In set-up n. 02 plate surface was ground (average roughness R_a of about 0.2-0.1 μm), while in set-up n.01 it was rough (R_a of about 3.2-1.6 μm). From Figure 5, that shows TEG power output P as a function of computed temperature difference (T_{HC}-T_{CC}), it is clear that the better contact between the surfaces of the TEG and heating and cooling structures that is guaranteed by higher surface quality allows TEG to work in better conditions. This fact results in a lower ε_S for set-up n. 01 with respect to n. 02 (see Table 4). It is also possible to define a relationship (linear in the first approximation) between plate surface average roughness R_a and TEG power production as a function of computed temperature difference.

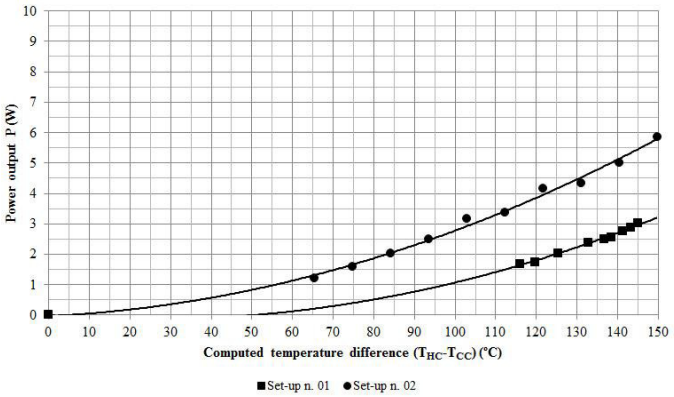

Fig. 5. TEG power output P as a function of computed temperature difference (T_{HC}-T_{CC}) for set-up n. 01 and set-up n. 02: comparison between different surface quality.

The reason for such a result lies in the contact resistance to heat flux from the hot to cold sides of the TEG. As long as consistency of contact is guaranteed, contact resistances are constant along the heat transfer surfaces. This fact produces a homogeneous heat flow along the surface of the TEG module, that is a homogeneous temperature distribution. However, when the contact resistances vary in a consistent manner, the heat flow will vary locally, with negative repercussions on the temperature distribution along the TEG module. Another parameter that influences

contact resistance is the TEG module compression rate. Figure 6 shows TEG power output P as a function of computed temperature difference (T_{HC}-T_{CC}) for test facility set-up from n. 08 to set-up n. 10. In these set-ups the only parameter that has been changed is module compression. As expected, the higher the compression rate, the higher the power output P and surface heat uniformity ε_S (see Table 4). So, compression must be kept as high as possible, compatibly with the compressive strength of the TEG, to better level contact resistance on the TEG surfaces.

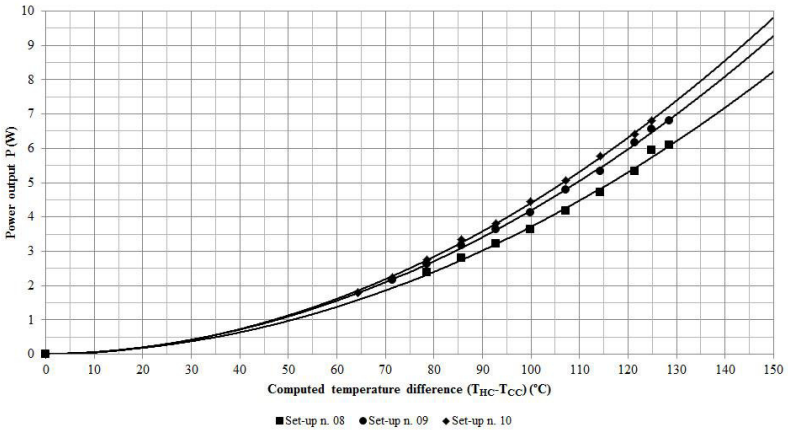

Fig. 6. TEG power output P as a function of computed temperature difference (T_{HC}-T_{CC}) from set-up n. 08 to set-up n. 10: comparison among different compression rate.

Ceramic wafers, aluminum plates and thermal grease were added to set-up in order to test their effect on surface heat uniformity ε_S. Naturally, the presence of these elements decreases conductivity factor ε_λ. An equilibrium must be found in order to optimize heat flux optimization through the TEG module without decreasing the TEG module working temperatures too much. In fact, from Equations 1, 3 and 4 the relationship between power output P and measured temperature T_H' and T_C' can be written as in Equation 5.

$$P = \frac{2m}{(1+m)^2}\frac{\alpha^2}{\rho}\frac{NA(T_H'-T_C')^2}{(L+n)(1+2rL_C/L)}\varepsilon_\lambda\varepsilon_S \tag{5}$$

As shown in Table 4, ceramic wafer presence contributes to increase surface heat uniformity ε_S: the value passes from 81.6% (set-up n. 02, without ceramic wafer) to 86.8% (set-up n. 07, with ceramic wafer). On the other hand, the conductivity factor ε_λ decreases respectively from 93.6% to 85.9%. So, if the two set-ups are matched in the same steady-state condition, no variation in power output is achieved by ceramic wafer addition to the system. Also aluminum plates and thermal grease presence (in addition to the ceramic wafer) has a good influence on surface heat uniformity ε_S. The value passes from 86.8% with set-up n. 07 to 91.8% with set-up n. 10. However, the conductivity factor ε_λ reduction from 85.9% to 71.4% produces a power output decrease if the two set-ups are matched in the same steady-state conditions. So, the addition of aluminum plates and thermal grease seems to be a good solution only when the heat source has a higher temperature than the TEG maximum working temperature and, thus, a temperature decrease on the TEG hot side is needed.

Figure 7 shows TEG power output P as a function of temperature difference ΔT on the TEG module for test facility set-up from n. 03 to set-up n. 06. In these tests the only parameter that has been changed is R_L. Power output P seems to increase with the R_L increase, while it could be expected that power output P is maximum at matched load (m=1), that is set-up n. 04. Actually, the result is in accordance with the literature: since the Peltier effect reduces the temperature difference across the TEG thermocouples, the effective inner resistance R at load condition is larger than the ohmic inner resistance without load [12,13].

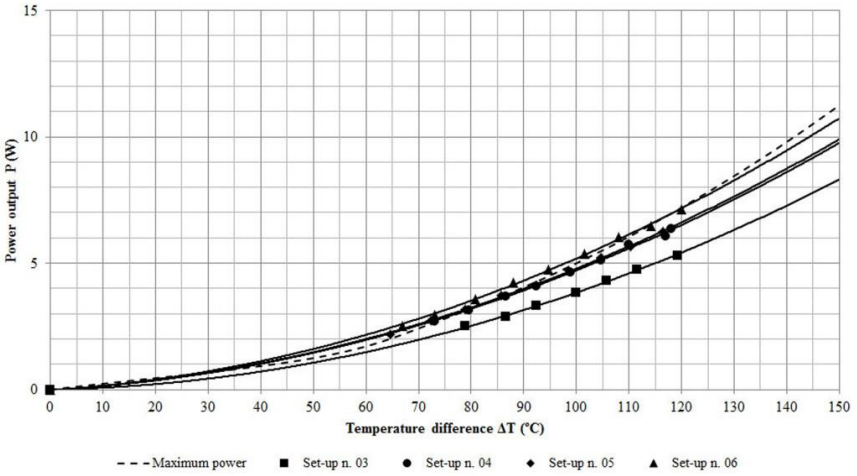

Fig. 7. TEG power output P as a function of ΔT from set-up n. 03 to set-up n. 06: comparison among different load electrical resistance.

Table 4. Conductivity factor ε_λ and surface heat uniformity factor ε_S for different test facility set-ups.

Test facility set-up	Conductivity factor ε_λ	Surface heat uniformity factor ε_S	$\varepsilon_\lambda \times \varepsilon_S$
01	93.6%	57.1%	53.4%
02	93.6%	81.6%	76.4%
03	85.9%	82.8%	71.1%
04	85.9%	82.0%	70.4%
05	85.9%	82.3%	70.0%
06	85.9%	84.6%	72.7%
07	85.9%	86.8%	74.6%
08	71.4%	84.4%	60.3%
09	71.4%	89.8%	64.1%
10	71.4%	91.8%	65.5%

Since heat exchange uniformity both on the cold and hot sides of the TEG module is a relevant parameter in designing TEG integration with a biomass boiler, the influence of the type of fluids used as heat carriers must be studied in greater detail.

5. Test facility up-grade

The theoretical and experimental analysis described in this paper highlights relevant criteria for industrial plant design. In particular, it was shown that the search for uniformity of heat distribution on TEG surfaces (expressed by ε_S) through the inclusion of additional materials does not introduce real benefits, as it is offset by the conductivity factor decrease (ε_λ). On the other hand, when more TEGs are connected in series, heat uniformity across TEGs surfaces becomes a relevant issue because the difference in TEG voltage output needs to be avoided in order to guarantee the highest performance. Therefore, to really obtain the benefits of the uniform heat distribution and its steadiness, without reducing TEG ΔT, an analysis on fluid characteristics must be done. In particular, the influence of specific heat on heat exchange is going to be investigated in depth, since at constant heat exchange and fluid flow, a specific heat increase means a temperature difference decrease, with relevant advantages in terms of heat flux homogeneity across TEG surfaces.

An innovative test facility for industrial application will be designed. Nine thermoelectric cells (HZ-20 module) will be connected in series in a single row and in parallel connection among three rows in order to provide an estimated total electric power of about 180 W (at 7.5 V and 24.5 A). The application to a biomass boiler will involve the use of a higher number of these modules in order to provide enough energy to the boiler auxiliary plant. So, an optimization process will also involve a biomass boiler: electric power consumption should be minimized through a dedicated design activity. For example, ventilation power consumption can be reduced by natural chimney draft, or water pumping consumption can be limited or eliminated thanks to a natural circulation system or by using an integrated steam pump.

6. Conclusion

This paper describes the experimental test results on a thermoelectric module (HZ-20 model) applied on a test facility, that simulates industrial boiler condition. In particular, TEG performance was analyzed as function of different parameters that affect electric power production, since energy conversion efficiency has a secondary role, because thermal power can be completely recovered on the sink side. Two different factors, one involving heat conductivity through the entire heating-cooling TEG system (conductivity factor ε_λ) and the other involving heat flow homogeneity through the TEG (surface heat uniformity factor ε_S), are defined in the paper and then analyzed. This experimental and theoretical analysis make it possible to realize a preliminary design of an innovative test facility that will study the opportunity to exploit the thermodynamic characteristics of different fluids in terms of exchange coefficient and temperature steadiness, to optimize both conductivity and surface heat uniformity factors. The test facility will be realized and then tested on an industrial biomass boiler of about 300 kW_{th}.

Acknowledgements

The research is financed by the Research and Development Department of HERA S.p.A.

References

[1] Saccani C, Bianchini A, Pellegrini M. On the use of renewable sources for energy production and integration with industrial plants (Sull'utilizzo di fonti rinnovabili per la produzione di energia e integrazione con impianti industriali, in Italian). Proceedings of XV International Ecomondo - Material and Energy Recovery and Sustainable Development. 9-12 November 2011, Rimini, Italy.

[2] Rowe DM, Min G. Evaluation of thermoelectric modules for power generation. J Power Sources 1998; 73: 193-8.

[3] Nuwayhid RY, Rowe DM, Min G. low cost stove-top thermoelectric generator for regions with unreliable electricity supply. Renewable Energy 2003; 28: 205-22.

[4] Min G, Rowe DM. Symbiotic application on thermoelectric conversion for fluid preheating/power generation. Energy Convers Manage 2004; 43: 221-8.

[5] Killander A, Bass J. A stove-top generator for cold areas. Proceedings of 15th International Conference on Thermoelectrics, pp. 390-393, Pasadena, Ca, USA, 1996.

[6] Nuwayhid RY, Shihadeh A, Ghaddar N. Development and testing of a domestic woodstove thermoelectric generator with natural convection cooling. Energy Conversion and Management 2005; 46: 1631-43.

[7] Nuwayhid RY, Hamade R. Design and testing of a locally made loop-type thermosyphonic heat sink for stove-top thermoelectric generators. Renew Energy 2005; 30: 1101-16.

[8] Lertsatitthanakorn C. Electrical performance analysis and economic evaluation of combined biomass cook stove thermoelectric (BITE) generator. Bioresource Technology 2007; 98: 1670-4.

[9] Champier D, Bedecarrats JP, Rivaletto M, Strub F. Thermoelectric power generation from biomass cook stoves. Energy 2010; 35: 935-42.

[10] Champier D, Bedecarrats JP, Kousksou T, Rivaletto M, Strub F, Pignolet P. Study of a TE (thermoelectric) generator incorporated in a multifunction wood stove. Energy 2011; 36: 1518-26.

[11] Pellegrini M. Advanced components for biomass combustion plants (Componentistica avanzata per impianti di combustione a biomassa, in Italian). PhD Thesis. AMS Acta, Bologna, Italy, 2012. ISSN: 2038-7954.

[12] Freunek M, Muller M, Ungan T, Walker W, Reindl LM. New physical model for thermoelectric generators. Journal of Electronic Materials 2009; 38: 1214-20.

[13] Casano G, Piva S. Experimental investigation of the performance of a thermoelectric generator based on Peltier cells. Experimental Thermal and Fluid Science 2011; 35: 660-9.